Enhancement of ductility of cold-deformed 316L stainless steel by electric pulse treatment

Ling Xue*, Ju* Huang, *Qiang* Li*, Mingxia* Wu*, *Jian* Liu*, and Yi* Yang

School of Mechanical Engineering, Sichuan University, Chengdu, 610065, PR China

Abstract. In this study, we performed electric pulse treatment (EPT) on the cold-deformed 316L stainless steel. The effects of EPT on the temperature rise characteristics, tensile properties and microstructure of cold-deformed 316L SS were investigated. The results show that changes in current density have a significant effect on the surface temperature and tensile properties. Compared with the UT samples, at a current density of 44 A/mm2, the elongation after fracture reached a peak of 39.8% (the enhancement rate is 14.4%), while the ultimate tensile strength of all the EPTed samples shows no significant change. Interestingly, although the sample experienced an increase in temperature during the EPT process, the phase composition and grain structure remained unchanged significantly. This implies that the improvement in the ductility of the samples may be attributed to the reduction of micropores. The present research provides new light to the enhancement of ductility of cold-deformed 316L stainless steel.

Keywords. 316L stainless steel, Electric pulse treatment, Tensile properties, Microstructure

1 Introduction

316L Stainless Steel (SS) is a typical austenitic stainless steel, which is widely used in aerospace, nuclear industry, energy and chemical industry, medical devices and other high-tech fields, for its excellent corrosion resistance and good comprehensive mechanical properties [1]. However, in the cold plastic forming process of the 316L SS, a large amount of strain and work hardening will be produced, resulting in a decrease in its ductility, which in turn affects the forming efficiency and the quality of the formed parts [2]. Conventional heat treatment can effectively solve these problems, but heat treatment often needs to be accomplished by a long period of heating and holding, which will cause a large amount of energy waste [3]. In recent years, studies have shown that electric pulse treatment (EPT) can rapidly enhance the ductility of cold-plastically deformed metals in a short period of time [4, 5]. Compared with conventional heat treatment, EPT has the advantages of convenient operation, high energy utilization rate and cleanliness and environmental protection [6, 7]. Our previous studies have also shown that EPT can enhance the elongation of cold-deformed

* Corresponding author: wumingxia@scu.edu.cn

copper alloys and aluminum alloys with high efficiency [8, 9]. Hence EPT is a promising method for improving the tensile properties of cold-deformed 316L SS.

In this work, cold-deformed 316L SS was subjected to EPT, and the effects of current density on the surface temperature, tensile properties and microstructure of the samples were investigated by temperature recorder, tensile testing machine, X-ray diffraction (XRD), optical microscopy (OM), scanning electron microscopy (SEM).

2 Experimental details

The material used in this work is commercial 316L SS with the nominal chemical composition (wt.%) 17.3 Cr, 11.4 Ni, 2.1 Mo, 0.36 Si, 1.42 Mn, 0.02 C, 0.02 S, 0.03 P, balance Fe. It was machined into dogbone-shaped tensile specimens with a gauge dimension of 2 mm × 6 mm × 10 mm, and then it was deformed by 50% tensile deformation. The EPT of the 316L SS samples was performed on a self-developed electric pulse generator. Fig. 1 (a) shows the schematic diagram of the EPT process, the sample is clamped between the two electrodes of the device, and the direction of current through the sample is parallel to its tensile direction. During the EPT process, the temperature of the sample surface was recorded in real time via a K-type thermocouple connected to a temperature data collector at a frequency of 100 times per second. The detailed parameters of the EPT are shown in Table 1. The ETM305D universal test machine (WANCE, China) was used to perform the tensile test at an average speed of 0.01 mm/s at room temperature, and the tensile fracture morphology was observed by scanning electron microscope (SEM; JSM-IT500HR). The phase constituents were determined by X-ray diffraction (XRD; EMPYREAN) using Cu-Kα radiation (λ = 1.54 Å). The metallographic images were observed with an optical microscope (OM; OLYMPUS).

Table. 1 The detailed parameters of the EPT.

Samples	Pulse-Width (ms)	Current density (A/mm^2)	Time (s)
UT	0	0	0
EPT40	10	40	180
EPT44	10	44	180
EPT48	10	48	180

3 Results and discussion

3.1 Temperature rise characteristics

The variations of surface temperature of cold-deformed 316L SS in the EPT process are shown in Fig. 1 (b), it can be seen that, in the EPT stage, The samples show a significant increase in temperature, which is mainly attributable to the pulsed current on the sample of the Joule heating effect [10].

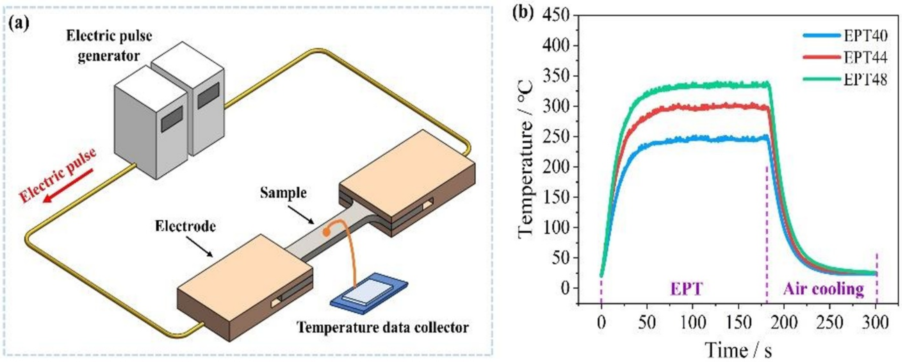

Fig. 1. (a) Schematic diagram of the EPT process. (b) Surface temperature of the cold-deformed 316L SS during the EPT process.

3.2 Tensile properties

The tensile properties of the samples before and after EPT are shown in Fig. 2. From Fig. 2 (b-d), it can be observed that compared with the UT samples, the ultimate tensile strength (UTS) of all the EPTed samples shows no significant change, while the elongation after fracture (EAF) and the product of strength and elongation (PSE = UTS × EAF) show different degrees of enhancement, and with the increase of the current density shows a trend of increasing firstly and then decreasing. At a current density of 44 A/mm2, the EAF and PSE show the largest enhancement rates, which are 14.4% and 15.5%, respectively. This means that EPT can increase the ductility of cold-deformed 316L SS while maintaining its strength.

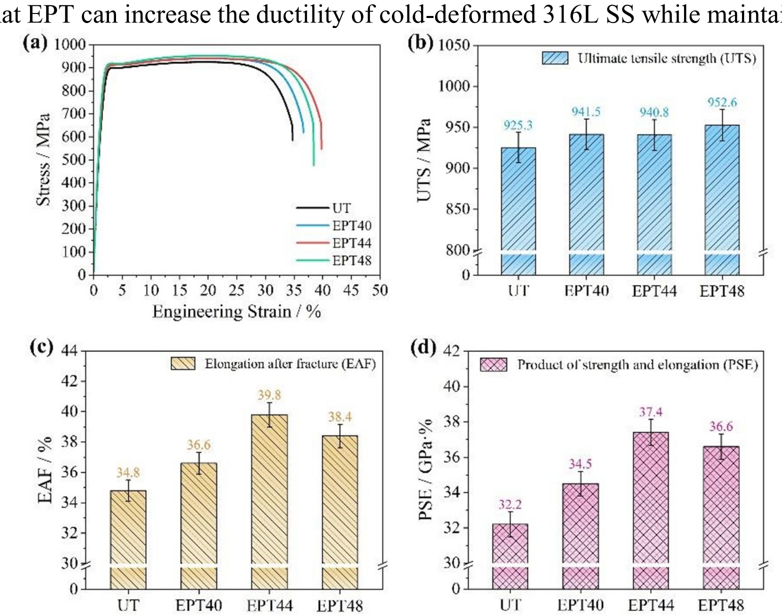

Fig. 2. The tensile properties of the cold-deformed 316L SS before and after EPT: (a) engineering stress-strain curves, (b) ultimate tensile strength, (c) elongation after fracture, (d) product of strength and elongation.

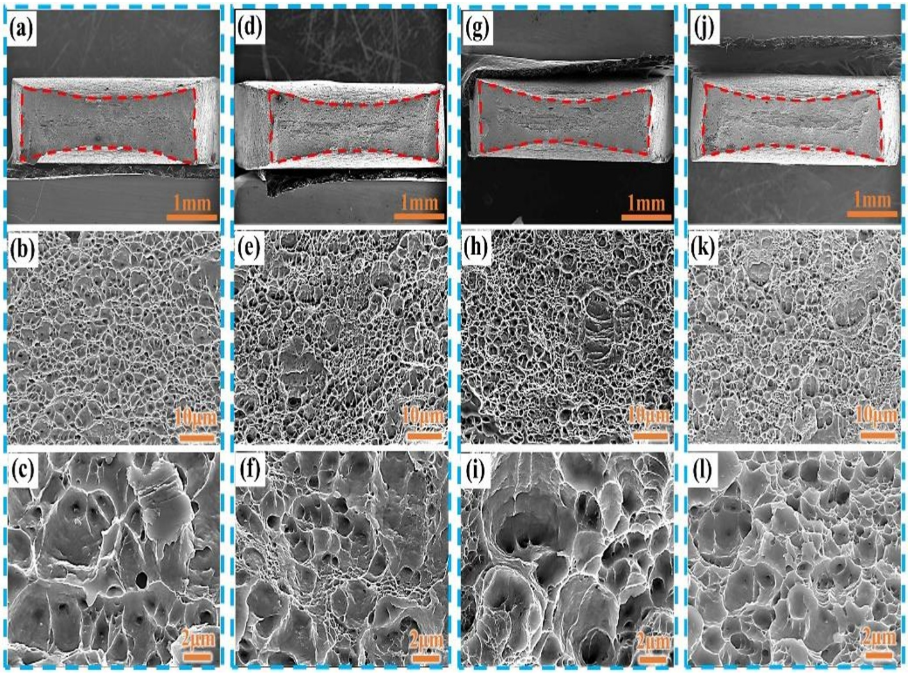

Fig. 3. Tensile fracture morphologies of cold-deformed 316L SS before and after EPT: (a-c) untreated, (d-f) EPT40, (g-i) EPT44, (j-l) EPT48.

The tensile fracture morphologies of cold-deformed 316L SS before and after EPT are shown in Fig. 3. It can be seen that all the tensile fractures show obvious necking phenomenon, which is typical of ductile fracture, and the corresponding section shrinkage is shown in Table 2. Moreover, the section shrinkage of all EPTed specimens is higher than that of UT one, and it exhibits a tendency to increase and then decrease with the increase of current density, and the maximum section shrinkage is observed at the current density of 44 A/mm2. It is observed further that the depth of the dimples of EPTed samples is larger than that of UT one, which shows a tendency to increase and then decrease with the increase of current density, and the depth of dimples is the largest when the current density is 44 A/mm2. These phenomena also indicate from another point of view that the EPT can effectively improve the ductility of cold-deformed 316L SS.

Table 2. The section shrinkage of the cold-deformed 316L SS before and after EPT.

Sample	UT	EPT40	EPT44	EPT48
Section shrinkage / %	63.48	64.07	67.89	65.93

3.3 Microstructure analysis

Fig. 4 (a-d) shows the OM images of the UT and EPTed samples. It can be seen that the grains of the cold deformed UT samples are mainly composed of equiaxed and twinned crystals, with slip lines distributing inside the grains. After EPT, the grain morphology does not change significantly. Fig. 4 (e) presents the XRD diffraction patterns of the UT and EPTed samples, the XRD patterns of all the specimens show obvious γ and α' characteristic peaks, and the intensity and diffraction angle of the peaks before and after EPT without significant changes. This is because, during the EPT process, the temperature of the sample is not greatly increased, while the treatment time is short, thus not enough to cause microstructure transformation. Therefore, the reason for the improvement in ductility may be consistent with our previous report [9], i.e., the EPT reduces the micropores in the cold-deformed samples, thereby enhancing the ductility.

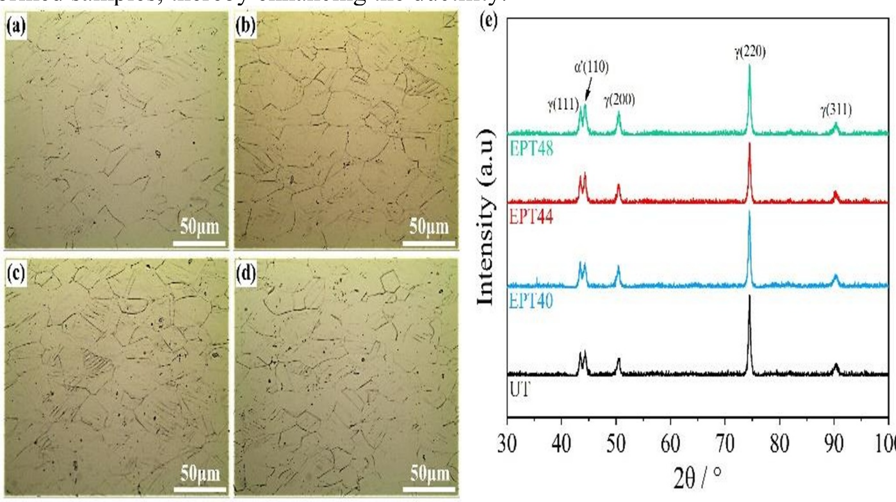

Fig. 4. (a-d) OM images of cold-deformed 316L SS before and after EPT: (a) untreated, (b) EPT40, (c) EPT44, (d) EPT48. (e) XRD diffraction patterns of cold-deformed 316L SS before and after EPT.

4 Conclusions

In summary, EPT can effectively improve the ductility of the cold-deformed 316L SS, and at a current density of 44 A/mm2, the elongation after fracture reached a peak of 39.8% (the enhancement rate is 14.4% compared with the untreated one), while the ultimate tensile strength of all the EPTed samples shows no significant change. Interestingly, although the sample experienced an increase in temperature during the EPT process, the phase composition and grain structure remained unchanged significantly. This implies that the improvement in the ductility of the samples may be attributed to the reduction of micropores.

The authors wish to acknowledge the financial support by the National Natural Science Foundation of China (Grant No. 52205490) and the Natural Science Foundation of Sichuan Province 2022NSFC0336.

References

1. Q. Mao, B. Gao, J. Li, Z. Huang, Y. Li, Mater. Sci. Technol., **35**, 1497-1503 (2019)
2. S. Kheiri, H. Mirzadeh, M. Naghizadeh, Mater. Sci. Eng., A, **759**, 90-96 (2019)
3. Q. Chao, S. Thomas, N. Birbilis, P. Cizek, P.D. Hodgson, D. Fabijanic, Mater. Sci. Eng., A, **821**, 141611 (2021)
4. Y.R. Ma, H.J. Yang, Y.Z. Tian, J.C. Pang, Z.F. Zhang, Mater. Sci. Eng., A, **713**, 146-150 (2018)
5. H. Xiao, S. Jiang, K. Zhang, Y. Jia, C. Shi, Z. Lu, J. Jiang, J. Alloys Compd., **814**, 152257 (2020)
6. T. Yu, D. Deng, G. Wang, H. Zhang, J. Cleaner Prod., **113**, 989-994 (2016)
7. W. Zeng, Y. Shen, N. Zhang, X. Huang, J. Wang, G. Tang, A. Shan, Scr. Mater., **66**, 147-150 (2012)
8. Y. Jiang, G. Tang, C. Shek, Y. Zhu, Z. Xu, Acta Mater., **57**, 4797-4808 (2009)

9. Q. Li, M. Wu, L. Xue, J. Huang, Z. Hu, G. Xu, C. Wu, X. Lou, Y. Yang, J. Mater. Sci., **59** (2024)
10. C. Liao, J. Huang, L. Xue, M. Wu, G. Yang, Y. Yang, Mater. Today Commun., **34**, 104969 (2023)
11. X. Wang, W. Dai, R. Wang, X. Tian, X. Zhao, J. Mater. Res., **29**, 975-980 (2014)